Terra Nova
THE EUROPEAN JOURNAL OF GEOSCIENCES

Insights from the Mw 6.3, 2009 L'Aquila earthquake (Central Apennines) to unveil new seismogenic sources through their surface signature: the adjacent San Pio Fault

Journal:	*Terra Nova*
Manuscript ID:	TER-2010-0051.R1
Wiley - Manuscript type:	Paper
Date Submitted by the Author:	n/a
Complete List of Authors:	Di Bucci, Daniela; Ufficio Rischio Sismico, Dipartimento della Protezione Civile Vannoli, Paola; Istituto Nazionale di Geofisica e Vulcanologia Burrato, Pierfrancesco; Istituto Nazionale di Geofisica e Vulcanologia Fracassi, Umberto; Istituto Nazionale di Geofisica e Vulcanologia Valensise, Gianluca; Istituto Nazionale di Geofisica e Vulcanologia
Keywords:	Seismotectonics, morphotectonics, active fault, San Pio basin, Italy

Insights from the M_w 6.3, 2009 L'Aquila earthquake (Central Apennines) to unveil new seismogenic sources through their surface signature: the adjacent San Pio Fault

Daniela Di Bucci[1]*, Paola Vannoli[2], Pierfrancesco Burrato[2], Umberto Fracassi[2] & Gianluca Valensise[2]

[1] - Dipartimento della Protezione Civile. Via Vitorchiano 4, 00189 Roma, Italy
[2] - Istituto Nazionale di Geofisica e Vulcanologia. Via di Vigna Murata 605, 00143 Roma, Italy

* Corresponding Author:
Daniela Di Bucci
Dipartimento della Protezione Civile
Via Vitorchiano, n. 4
00189 – Roma
Italy
tel.: ++39-06-68204761
e-mail: daniela.dibucci@protezionecivile.it

Key words

Seismotectonics, morphotectonics, active fault, San Pio basin, Italy

Running title

Surface signature of L'Aquila seismogenic faults

Abstract

We analyzed a broad region around L'Aquila in search of seismogenic faults similar to that responsible for the 6 April 2009 earthquake (M_w 6.3). Having the lessons learned from this earthquake in mind, we focused on adjacent areas displaying similar morphotectonic, geological and structural evidence. The basin running from Barisciano to Civitaretenga-Navelli, notably located near the southeastern edge of the 2009 aftershock pattern, appears to be one of such areas. We collected morphotectonic and structural data indicating that this basin is underlain by a major active normal fault (San Pio Fault). All the observations are very much reminiscent of the morphotectonic, geological and structural setting of area struck by the L'Aquila earthquake, suggesting that the newly identified fault has the potential for a M_w 6.2-6.4 shock.

Introduction

The 6 April 2009 L'Aquila earthquake (M_w 6.3) struck a portion of the Central Apennines (Italy; Fig 1) whose seismotectonic setting was believed to be especially well known. In fact, the earthquake caught most of the geological community by surprise. In the past, most of the attention was given to a number of range-bounding active faults displaying bedrock scarps up to 5 km in length; these were believed to be the surface expression of deep faults having a high seismogenic potential (e.g., Galadini *et al.*, 2000a; ITHACA Working Group, 2000; Walters *et al.*, 2009). In contrast, the source of the 6 April earthquake projects to the surface along the Paganica Fault, a tectonic element having a subdued surface expression which had been previously identified only by a minority of workers.

In the Central Apennines, the geometric and dimensional relationships of the deep seismogenic sources with the overlying surface faults have been the object of a lively debate for at least a decade. According to some workers (Valensise, 2009), previous investigators failed to identify the proper hierarchical relationships among all active faults occurring in the L'Aquila region, and even the surface expression of the fault responsible for the 6 April earthquake is at least controversial (e.g. EMERGEO Working Group, 2010).

The region is undergoing SW-NE extension (D'Agostino *et al.*, 2001; Serpelloni *et al.*, 2005) and is affected by earthquakes with magnitude up to 6.8 according to the historical earthquake catalogues (CPTI Working Group, 2004). Several investigators have mapped the numerous active faults of the region (e.g., Vezzani and Ghisetti, 1998; Galadini and Galli, 2000; Galadini *et al.*, 2000a, b; ITHACA Working Group, 2000; Roberts and Michetti, 2004; Akinci *et al.*, 2009; Boncio *et al.*, 2009; all with references). These are mostly extensional and SW-dipping, but for many of them no consensus exists concerning the state of activity and hence the relevance for the seismic hazard. Similarly to the surface faults, all seismogenic sources proposed in the literature prior to the L'Aquila earthquake dip to the SW and display extensional kinematics (Pace *et al.*, 2006; Akinci *et al.*, 2009; DISS Working Group, 2009; all with references). The location, geometry and kinematics of the L'Aquila seismogenic source match the current seismotectonic understanding of this part of the Central Apennines (Atzori *et al.*, 2009; Chiarabba *et al.*, 2009; Walters *et al.*, 2009; Fig. 1).

Is the apparent mismatch between the deep seismogenic source and its surface expression a permanent characteristic of this region? The exceptional wealth of data available for the L'Aquila earthquake provides important clues for addressing this question and for identifying potential seismogenic sources in the quiescent region located to the southeast of the 2009 rupture.

Lessons learned from the 6 April 2009 L'Aquila earthquake

Instrumental data show that the L'Aquila earthquake was caused by slip along a N130°-140°–striking, 40°-50°–dipping, 12-19 km–long normal fault located between 1-3 and 12-14 km depth (Atzori *et al.*, 2009; Chiarabba *et al.*, 2009; Walters *et al.*, 2009; Fig. 1). The surface strains induced by the L'Aquila source appear to fit rather convincingly most of the recent geological and morphotectonic features of the region, suggesting that these are the result of sustained slip over the fault plane that ruptured on 6 April. For instance, the pattern of coseismic subsidence revealed by InSAR analyses (Fig. 1) fits quite well the active depocenter of the Quaternary basin in the Aterno River valley near L'Aquila, peaking at ca. -25 cm, and minor reactivations of surface faults were observed coincident with the steepest gradients of the vertical coseismic strains. Brittle coseismic deformation includes free faces along bedrock fault scarps, faulting along synthetic splays, and fissures with or without slip; the maximum reported throw and opening are 10 cm and 12 cm, respectively, but in the average they do not exceed 3-5 cm (Boncio *et al.*, 2010). This pattern of rather subdued deformation is the expression of about 1 m slip over a fault having its uppermost tip at 1-3 km depth. Contrary to pre-2009 expectations, the 6 April earthquake did not cause a major reactivation of any of the large faults known in the area.

Having these lessons in mind, we focused on converging morphotectonic, geological and structural evidence, including (in descending order of importance):

- a N130°–elongated, ca. 15 km–long, actively subsiding depression, filled by Pleistocene and Holocene fluvial and lacustrine deposits;
- a characteristic drainage pattern and architecture of deposits suggesting that the basin is controlled by a large and relatively deep fault;
- a slowly uplifting range bounding the NE flank of the basin;
- a barely visible, SW–dipping, normal fault system, formed by a set of fractures and subtle, 60°-70°–dipping, synthetic and antithetic normal faults, located between the basin and the range and affecting Pleistocene-to-Holocene deposits.

We aim at demonstrating that these lines of evidence are suggestive of sustained slip over a seismogenic fault similar to the 6 April rupture, and hence are the key to unveil new seismogenic sources. Consideration of the relationships between coseismic surface strains and long-term geologic and landscape features is the only way of avoiding the inherent ambiguities carried by observations of brittle shallow faulting, thus allowing for a reliable identification of the surface expression of seismogenic faulting.

Working hypothesis

We analyzed the region around L'Aquila in search of seismogenic faults similar to that responsible for the 6 April 2009 earthquake (if any), focusing specifically on the southeastern end of the earthquake sequence. Coseismic and postseismic stress changes caused by slip along a normal fault are known to increase stress on other faults located along its strike (Nostro *et al.*, 2001). Following the L'Aquila earthquake, increased activity was recorded near Campotosto Lake, to the northwest of the 6 April rupture (Chiarabba *et al.*, 2009; Fig. 1), whereas to the southeast the number of aftershocks drops abruptly, suggesting that, if the seismogenic zone that generated the L'Aquila earthquake continues in this direction, it is currently locked. This observation, coupled with the known tendency of strong Apennines earthquakes to come in clusters (e.g. Guidoboni *et al.*, 2007 and Table 3 in Burrato and Valensise, 2008), prompted us to focus specifically on that reach of the seismogenic zone.

Based on our own field observations aided by the most recent geological maps (Vezzani and Ghisetti, 1998; Servizio Geologico d'Italia, 2006; Vezzani et al., 2009) we identified a zone that exhibits clear and multiple indications of current tectonic activity. This zone corresponds to the basin running from Barisciano to Civitaretenga-Navelli (Figs 1 and 2; hereinafter San Pio basin) and is notably situated near the southeastern edge of the 2009 aftershock pattern.

Overall the San Pio basin makes a good candidate for the long-term expression of a seismogenic fault comparable to the source of the L'Aquila earthquake. It has an active, marshy depocenter located in its central part (Figs 2 and 4). The literature reports a faintly visible, SW-dipping, normal fault system between the basin and the range, reactivated during the Pleistocene and currently active (Fig. 1; Vezzani and Ghisetti, 1998; Roberts and Michetti, 2004).

To verify our hypothesis we carried out a morphotectonic analysis based on remote sensing and field surveys, and compared the results with the Quaternary geology of the San Pio basin. This comparison subsequently drove the structural analysis in the field.

Morphotectonic analysis

According to the literature (Servizio Geologico d'Italia, 2006), the Quaternary deposits filling the San Pio basin can be subdivided into three main units dated to the Pliocene (?)-Middle Pleistocene, Upper Pleistocene and Holocene, respectively (AP, VM and Hol in Fig. 3). These ages are based on regional correlation and, in this framework, on depositional relationships, pedogenic soil development, tephra correlation, radiometric dating, and inferences on climatic control on sedimentation. These continental deposits are topped by several terraced surfaces; the ones we recognized in the western part of the study area lie at the top of the Pliocene (?)-Middle Pleistocene

deposits (Fig. 4). Quaternary deposits range from colluvial and coarse alluvial facies along the basin slopes to fine alluvial and lacustrine facies in the valley.

The basin is visibly asymmetric, its NE slope being steeper (Fig. 5). We interpret this asymmetry as tectonic in origin, as suggested by the general northeastward tilt of the Pleistocene terraced surfaces. Tilting also affects surfaces at the top of Holocene deposits and can be recognised on both sides of the axial drainage, showing that it persists through time and is independent from the fluvial evolution of the basin. The active depocenter of the basin is located in its central part in the middle of the plain and shifted north-eastwards toward the village of San Pio delle Camere, at a site traditionally named “il Lago” (the Lake; Figs. 4 and 5), where Holocene silty-clayey deposits are found.

Structural analysis

Tilting of the Quaternary surfaces suggests that a major active fault could be located along the NE slope of the San Pio Basin. The structural analysis carried out revealed that Pleistocene continental deposits are affected by mesoscale brittle deformation only at specific sites roughly located at mid-slope elevation. These sites (**a** to **f** in Figs 4 and 6) are aligned and all exhibit normal faulting along NW-SE surfaces.

Along the westernmost part of the slope (Fig. 6**a**), a N140°-65° fault plane is seen to cut Middle Pleistocene deposits. A ca. 30 m-wide damage breccia affects SW-dipping layers in the hanging wall, whereas bedding in the footwall dips to the NE. Moving to the SE of Barisciano, Middle Pleistocene deposits exposed in a narrow creek (Fig. 6**b**) are cut by a ca. 10 m–wide, quite complex set of SW-dipping faults, accompanied by minor NE-dipping antithetic faults. Their strike and dip are in the range N120°-N165° and 45°-75°, respectively. Further to the SE (Fig. 6**c**), a 4 m–wide fault zone occurs, bounded to the SW by a N130°-80° fault plane and to the NE by a N300°-65° plane. The bedding of Middle Pleistocene deposits dips 11°-20° to the SW but disappears completely within the fault zone.

The best evidence for this fault zone is found very close to San Pio delle Camere (Figs 6**d** and 7), where quarry works unearthed a large fault plane oriented N150°-50° and having a pitch of 105°. The footwall of this fault is formed by Mesozoic oolithic limestone (Fig. 7b); the hanging wall hosts Middle Pleistocene and Upper Pleistocene slope deposits that are displaced by numerous fault planes striking N120°-N135° and dipping 48°-80°. A relatively large fault exposed in the most distant portion of the hanging wall shows clear Late Pleistocene and probable Holocene activity (Fig. 7a). We observe over-thickening of the Upper Pleistocene deposits on the fault hanging wall, which implies faulting during sedimentation. Moreover, the top part of these deposits, that does not

show syntectonic over-thickening, is faulted up to the topographic surface (i.e. the fault is not sealed). We conclude that the fault acted both during and after the deposition of the Upper Pleistocene deposits, thus implying probable Holocene activity. A similar reasoning can be used for the thickness and distribution of the Middle Pleistocene deposits with respect to the fault having its footwall in bedrock: thus this latter fault certainly slipped during and after the Middle Pleistocene. In summary, the data collected at site **d** show that the investigated normal fault set has developed since the Middle Pleistocene and is currently active.

Two additional sites (Fig. 6**e** and **f**) located near the easternmost end of the basin slope display well exposed fault planes with Mesozoic limestone at the footwall and Upper Pleistocene deposits at the hanging wall. The fault set near Civitaretenga (Fig. 6**e**) is composed by some N110°-63°–oriented surfaces, whereas the fault near Navelli (Fig. 6**f**) strikes N160°-165° and dips 55°-60° with pitch of 90°. We checked that motion affecting the faults described above cannot be ascribed to gravitational causes, for instance landslides. In the last two cases, however, we cannot rule out the exhumation of pre-existing faults; if compared with the other faults described, however, the location, geometry and kinematics of these faults suggest that they can be activated as part of the same fault system.

Results and Discussion

We believe the data we collected satisfy our working hypothesis, indicating that the San Pio basin is underlain by a major active normal fault, hereinafter San Pio Fault. Table 1 summarizes the fault parameters that fit best the available data, obtained using empirical relationships (Wells and Coppersmith, 1994). We checked the geometry and kinematics of the model fault through a simple elastic dislocation theory approach modified to account for interseismic non-elastic readjustments of the upper crust (Valensise and Ward, 1991; Figure 8). We compared the topographic changes that are expected to result from sustained slip on the proposed fault with a set of topographic profiles crossing the San Pio basin (Fig. 5). There exists a good agreement between the expected subsidence patterns and (i) the basin asymmetry, (ii) the location of the maximum long-term subsidence, and (iii) the northeastward tilt of the terraced surface remnants in the valley. Moreover, the surface projection of the model fault coincides with the location of the active faults described in the previous section. Further analyses could provide more precise ages for the faulted deposits, thus allowing slip rate to be estimated.

What we observed in the study area is very much reminiscent of the morphotectonic, geological and structural evidence available for the L'Aquila earthquake, suggesting that the newly

identified fault is potentially seismogenic. Empirical relationships (Wells and Coppersmith, 1994) show that the San Pio Fault may generate M_w 6.2-6.4 earthquakes.

Galli et al. (2010) suggest that the Paganica fault can slip both alone, as in 2009, or along with adjacent faults in much larger earthquakes. In principle, a comparable behavior cannot be ruled out for the San Pio fault. At the moment, however, neither is geological evidence available for such a "non-characteristic" style, nor are M>6.3 historical earthquakes known to have occurred in the San Pio basin. Therefore, we conservatively associate M_w 6.2-6.4 earthquakes to the San Pio fault.

Finally, to assess whether the San Pio fault may generate an earthquake soon we must answer to two independent questions:

- did stress changes caused by the 2009 earthquake bring the San Pio Fault closer to failure?
- when did the San Pio fault last rupture its entire length?

According to Walters et al. (2009), the 2009 earthquake did increase the stress level on the San Pio Fault, therefore bringing it closer to failure. Answering the second question requires consideration of the local historical earthquakes. According to the CFTI4Med catalogue (Guidoboni et al., 2007), over the past 7 centuries the area located southeast of L'Aquila has been hit by three significant earthquakes (Fig. 8):

- 1315, 3 December (M 5.7), a poorly documented earthquake that is known to have generically damaged "the L'Aquila castles";
- 1461, 27 November (M 6.3), similar in strength to the 2009 but difficult to locate precisely due to the small number of intensity data, possibly reflecting an overlap with the effects of the 1456 earthquake, on the northern slope of the Maiella Massif;
- 1762, 6 October (M 6.0), that struck all villages around the San Pio basin.

The 1461 and 1762 damage distributions are rather similar to that of the 2009 earthquake but shifted towards the southeast by a few km (Fig. 8). Overall the accuracy of the available locations does not allow any of these earthquakes to be assigned to the 6 April or to the San Pio Fault beyond mere speculation. Paleoseismological investigations currently underway (Pantosti et al., 2010) may help in assigning one or more of these events to the 6 April fault, and indirectly to the San Pio Fault.

Acknowledgments

We gratefully thank Karl Wegmann and Pilar Villamor for their careful reviews. This research benefited from funding provided by the Italian Presidenza del Consiglio dei Ministri – Dipartimento della Protezione Civile (DPC). Scientific papers funded by DPC do not represent its official opinion and policies.

References

Akinci, A., Galadini, F., Pantosti, D., Petersen, M., Malagnini, L. and Perkins, D., 2009. Effect of Time Dependence on Probabilistic Seismic-Hazard Maps and Deaggregation for the Central Apennines, Italy. *Bulletin of the Seismological Society of America*, **99** (2A), 585–610.

Atzori, S., Hunstad, I., Chini, M., Salvi, S., Tolomei, C., Bignami, C., Stramondo, S., Trasatti, E., Antonioli, A. and Boschi, E., 2009. Finite fault inversion of DInSAR coseismic displacement of the 2009 L'Aquila earthquake (central Italy). *Geophysical Research Letters*, **36**, L15305, doi:10.1029/2009GL039293

Bigi, G., Coli, M., Cosentino, D., Parotto, M., Praturlon, A., Sartori, R., Scandone, P. and Turco, E., 1992. Structural Model of Italy, Sheet 4, scale 1: 500,000. C.N.R. *Quaderni de ''La Ricerca Scientifica''*, **114**. Monografie finali, Progetto finalizzato ''Geodinamica'', 3.

Boncio P., Pizzi, A., Brozzetti, F., Pomposo, G., Lavecchia, G., Di Naccio, D. and Ferrarini, F., 2010. Coseismic ground deformation of the 6 April 2009 L'Aquila earthquake (central Italy, Mw6.3). *Geophysical Research Letters*, **37**, L06308, doi:10.1029/2010GL042807

Burrato, P. and Valensise, G., 2008. Rise and fall of a hypothesized seismic gap: source complexity in the Mw 7.0 16 December 1857 Southern Italy earthquake. *Bulletin of the Seismological Society of America*, **98**, 139-148, doi: 10.1785/0120070094.

Boncio, P., Tinari, D.P., Lavecchia, G., Visini, F. and Milana, G., 2009. The instrumental seismicity of the Abruzzo Region in Central Italy (1981-2003): Seismotectonic Implications. *Ital. J. Geosci. (Boll. Soc. Geol. It.)*, **128** (2), 367-380.

Chiarabba, C., Amato, A., Anselmi, M., Baccheschi, P., Bianchi, I., Cattaneo, M., Cecere, G., Chiaraluce, L., Ciaccio, M.G., De Gori, P., De Luca, G., Di Bona, M., Di Stefano, R., Faenza, L., Govoni, A., Improta, L., Lucente, F.P., Marchetti, A., Margheriti, L., Mele, F., Michelini, A., Monachesi, G., Moretti, M., Pastori, M., Piana Agostinetti, N., Piccinini, D., Roselli, P., Seccia, D. and Valoroso, L., 2009. The 2009 L'Aquila (central Italy) MW6.3 earthquake: main shock and aftershocks. *Geophysical Research Letters*, **36**, L18308, doi:10.1029/2009GL039627

CPTI Working Group, 2004. *Catalogo Parametrico dei Terremoti Italiani, versione 2004 (CPTI04)*. INGV, Bologna. http://emidius.mi.ingv.it/CPTI/

D'Agostino, N., Giuliani, R., Mattone, M. and Bonci, L., 2001. Active crustal extension in the central Apennines (Italy) inferred from GPS measurements in the interval 1994-1999. *Geophysical Research Letters*, **28** (10), 2121-2124.

DISS Working Group, 2009. *Database of Individual Seismogenic Sources (DISS), Version 3.1.0: A compilation of potential sources for earthquakes larger than M 5.5 in Italy and surrounding areas*. http://diss.rm.ingv.it/diss/, © INGV 2009 - Istituto Nazionale di Geofisica e Vulcanologia - All rights reserved.

EMERGEO Working Group, 2010. Evidence for surface rupture associated with the Mw 6.3 L'Aquila earthquake sequence of April 2009 (central Italy). *Terra Nova*, **22**, 43-51.

Galadini, F. and Galli, P., 2000. Active Tectonics in the Central Apennines (Italy) – Input Data for Seismic Hazard Assessment. *Natural Hazards*, **22**, 225-270.

Galadini, F., Meletti, C. and Rebez, A., Eds, 2000a. *Le ricerche del GNDT nel campo della pericolosità sismica (1996-1999)*. CNR-Gruppo Nazionale per la Difesa dai Terremoti, Roma, 397 pp.

Galadini, F., Messina, P. and Sposato, A., 2000b. Tettonica quaternaria nell'Appennino centrale e caratterizzazione dell'attività di faglie nel Pleistocene superiore-Olocene. In: *Le ricerche del GNDT nel campo della pericolosità sismica (1996-1999)* (Galadini, F., Meletti, C. and Rebez, A., eds). CNR-GNDT, Roma, 181-192.

Galli, P., Giaccio, B. and Messina, P., 2010. The 2009 central Italy earthquake seen through 0.5 Myr-long tectonic history of the L'Aquila faults system. *Quaternary Science Reviews*, xxx, 1-22.

Gruppo di Lavoro CPTI, 2004. *Catalogo Parametrico dei Terremoti Italiani, versione 2004 (CPTI04)*. INGV, Bologna, http://emidius.mi.ingv.it/CPTI/

Guidoboni, E., Ferrari, G., Mariotti, D., Comastri, A., Tarabusi, G. and Valensise, G., 2007. *CFTI4Med, Catalogue of Strong Earthquakes in Italy (461 B.C.-1997) and Mediterranean Area (760 B.C.-1500)*. INGV-SGA. Available from http://storing.ingv.it/cfti4med/

Hanks, T. and Kanamori, H., 1979. A moment magnitude scale. *J. Geophys. Res.*, **84** (B5), 2348-2350.

ISIDe, 2010. *Italian Seismic Instrumental and parametric Data-basE*. http://iside.rm.ingv.it/iside/standard/index.jsp. © Italian Seismic Bulletin, Istituto Nazionale di Geofisica e Vulcanologia - All rights reserved.

ITHACA Working Group, 2000. *ITaly HAzard from CApable faults*. Servizio Geologico d'Italia-ISPRA. On-line database (http://www.isprambiente.it/ithaca/)

Nostro, C., Piersanti, A. and Cocco, M., 2001. Normal fault interaction caused by cosismic and postseismic stress changes. *Journal of Geophysical Research*, **106**, 19,391-19,410.

Pace, B., Peruzza, L., Lavecchia, G. and Boncio, P., 2006. Layered Seismogenic Source Model and Probabilistic Seismic-Hazard Analyses in Central Italy. *Bulletin of the Seismological Society of America*, **96** (1), 107-132.

Pantosti, D., Cinti, F.R., De Martini, P.M., Pucci, S., Civico, R., Pierdominici, S., Cucci, L., Brunori, C.A., Patera, A. and Pinzi, S., 2010. Discovering the characteristics of the surface faulting ancestors of the L'Aquila April 6, 2009 earthquake by paleoseismological investigations. *Geophysical Research Abstracts*, **12**, EGU2010-9673.

Roberts, G.P. and Michetti, A.M., 2004. Spatial and temporal variations in growth rates along active normal fault systems: an example from The Lazio–Abruzzo Apennines, central Italy. *Journal of Structural Geology*, **26**, 339-376.

Serpelloni, E., Anzidei, M., Baldi, P., Casula, G. and Galvani, A., 2005. Crustal velocity and strain rate fields in Italy and surrounding regions: new results from the analysis of permanent and nonpermanent GPS networks, *Geophys. J. Int.,* **161**, 861-880, doi: 10.1111/j.1365-246X.2005.02618.x.

Servizio Geologico d'Italia, 2006. *Geological Map of Italy*. 1:50,000 scale. Sheets n. 359 L'Aquila and n. 360 Torre de' Passeri.

Scognamiglio, L., Tinti, E., Michelini, A., Dreger, D., Cirella, A., Cocco, M., Mazza, S. and Piatanesi, A., 2010. Fast Determination of Moment Tensors and Rupture History: Application to the April 6th 2009, L'Aquila Earthquake. *Seismological Research Letters*, **81** (6), 892-906, DOI: 10.1785/gssrl.81.6.892

Valensise, G., 2009. Faglie attive e terremoti: tempo di cambiare strategie. *Geoitalia*, **28**, 12-17. doi: 10.1474. Available on-line: http://www.geoitalia.org/upload/home_page/geoitalia/n28.pdf

Valensise, G. and Ward, S., 1991. Long-term uplift of the Santa Cruz coastline in response to repeated earthquakes along the San Andreas Fault. *Bulletin of the Seismological Society of America*, **81**, 1694-1704.

Vezzani, L., Festa, A. and Ghisetti, F., 2009. *Geological-structural map of the Central-Southern Apennines (Italy)*. 1:250,000 scale. S.E.L.CA. ed., Firenze.

Vezzani, L. and Ghisetti, F., 1998. Carta Geologica dell'Abruzzo, 1:100,000 scale. S.E.L.CA. ed., Firenze.

Walters, R.J., Elliott, J.R., D'Agostino, N., England, P.C., Hunstad, I., Jackson, J.A., Parsons, B., Phillips, R.J. and Roberts, G., 2009. The 2009 L'Aquila earthquake (central Italy): A source mechanism and implications for seismic hazard. *Geophysical Research Letters*, **36**, L17312, doi:10.1029/2009GL039337

Wells, D.L., and Coppersmith, K.J., 1994. New empirical relationships among magnitude, rupture length, rupture width, rupture area, and surface displacement. *Bull. Seismol. Soc. Am.*, **84**, 974-1002.

Figure captions

Fig. 1

Simplified geological map of the Central Apennines (from Bigi *et al.*, 1992; redrawn and modified). Legend: 1. Quaternary continental deposits; 2. Pliocene foredeep deposits; 3. Miocene foredeep deposits; 4. Meso-Cenozoic marine deposits of the Central Apennines chain; 5. Main thrust fronts; 6. active faults according to Vezzani and Ghisetti (1998; thin when uncertain); 7. Large star: 2009 mainshock epicenter; small stars: epicenters of largest aftershocks of 2009 sequence (ISIDe, 2010); 8. L'Aquila earthquake sequence (1 April-31 July, 2009; data from ISIDe, 2010); 9. Interferometric fringes illustrating elevation changes induced by the L'Aquila earthquake (from Walters *et al.*, 2009, redrawn); 10. Surface projection of the mainshock fault rupture (from Table 1 in Walters *et al.*, 2009, redrawn). **2a** and **2b**: view points of pictures in Fig. 2. Focal mechanisms of the mainshock and the two largest aftershocks are from Scognamiglio *et al*. (2010).

Fig. 2

Views of the San Pio basin. **a.** Picture taken from the northwestern end of the basin, view to the southeast. **b.** Picture taken from the southeastern end of the basin, view to the northwest. See Fig. 1 for location of the view points.

Fig. 3

Geological setting of the study area (after Servizio Geologico d'Italia, 2006, redrawn and modified). Continental deposits: AP) Pliocene (?)-Middle Pleistocene; CA) latest Middle Pleistocene; VM) Upper Pleistocene; Hol) Holocene. Meso-Cenozoic bedrock is shown in grey. The black box represents the surface projection of the mainshock fault rupture (from Table 1 in Walters *et al.*, 2009, redrawn). The continental Quaternary deposits filling the San Pio basin are characterized by different facies. Talus breccias and alluvial fans crop out along the surrounding slopes. Toward the valley, these facies are interfingered with fluvial and lacustrine sediments, which fill the lower part of the basin. Both the talus breccias and the alluvial fan deposits occasionally exhibit a very coarse clastic texture, in the latter case formed by well rounded pebbles, and are locally rather thick, up to tens of meters. Silts and clays instead prevail in the lacustrine facies.

Fig. 4

Detail of Fig. 3. Hol-s marks the Holocene lacustrine facies. Notice that these deposits are found only in the central part of the basin, near the current depocenter, supporting the hypothesis that

subsidence has been a persisting feature throughout the Holocene. T1 to T3 are terraces at the top the AP deposits. Letters in white circles refer to the sites of structural analysis shown in Fig. 6.

Fig. 5

NNE-SSW-striking topographic profiles across the San Pio basin (traces in Fig. 4) and elevation changes due to 1 m of hypothetical slip over the model fault (in orange). Notice the asymmetry of the basin and the tilt towards NNE of the Pleistocene and Holocene surfaces, in accordance with the elevation changes predicted by the model. H: elevation a.s.l.; EVD: expected vertical displacement.

Fig. 6

Faults (red arrows) and fractures along the slope bounding the San Pio basin to the NE. See Fig. 4 for location of the sites of observation. Pliocene (?)-Middle Pleistocene and Upper Pleistocene continental deposits overlying Jurassic and Cretaceous limestones (Servizio Geologico d'Italia, 2006) crop out extensively. The Pleistocene deposits exhibit slope talus facies, in many cases characterized by a coarse texture with large calcareous blocks, but in some instances show fluvial facies with well rounded pebbles.

Fig. 7

Active faults bounding the central part of the San Pio basin to the NE, near the village of San Pio delle Camere (detail of the site 6d in Fig. 6). The faults slipped during and after the deposition of both the Pliocene (?)-Middle Pleistocene deposits (AP) and the Upper Pleistocene (VM) deposits.

Fig. 8

Plan view and cross-section of the seismogenic fault modeled for the San Pio basin (parameters in Table 1). Cross-section surface data from Servizio Geologico d'Italia (2006). The orange isolines show the expected elevation changes, in increments of 2 cm, resulting from 1 m of hypothetical unitary slip on the modeled fault (see also Fig. 5 for a cross-section view). Notice the good correspondence with basin geometry. The distribution of the L'Aquila aftershocks (green dots; ISIDe, 2010) and historical earthquakes (white squares; Guidoboni *et al.*, 2007) is also shown. Red stars: epicenters of the mainshock and of the largest aftershock of the 2009 L'Aquila sequence. As an example, the damage distribution of the 1762 Aquilano earthquake is shown in MCS intensity scale.

Table 1. San Pio Fault parameters

Location [Lat/Lon]	42.27/13.62	Based on geological data
Length [km]	16.2	Based on geological data
Width [km]	10.5	Calculated using the relationships from Wells and Coppersmith (1994)
Min depth [km]	0.7	Based on geological and geomorphological observations
Max depth [km]	8.7	Derived from dip, width and min depth
Strike [deg]	127	Based on geological and geomorphological observations
Dip [deg]	50	Based on geological and geomorphological observations
Rake [deg]	270	Based on geological and geomorphological observations
Slip [m]	0.5	Calculated using the relationship from Hanks and Kanamori (1979)
Magnitude [Mw]	6.2	Calculated using the relationship from Hanks and Kanamori (1979)

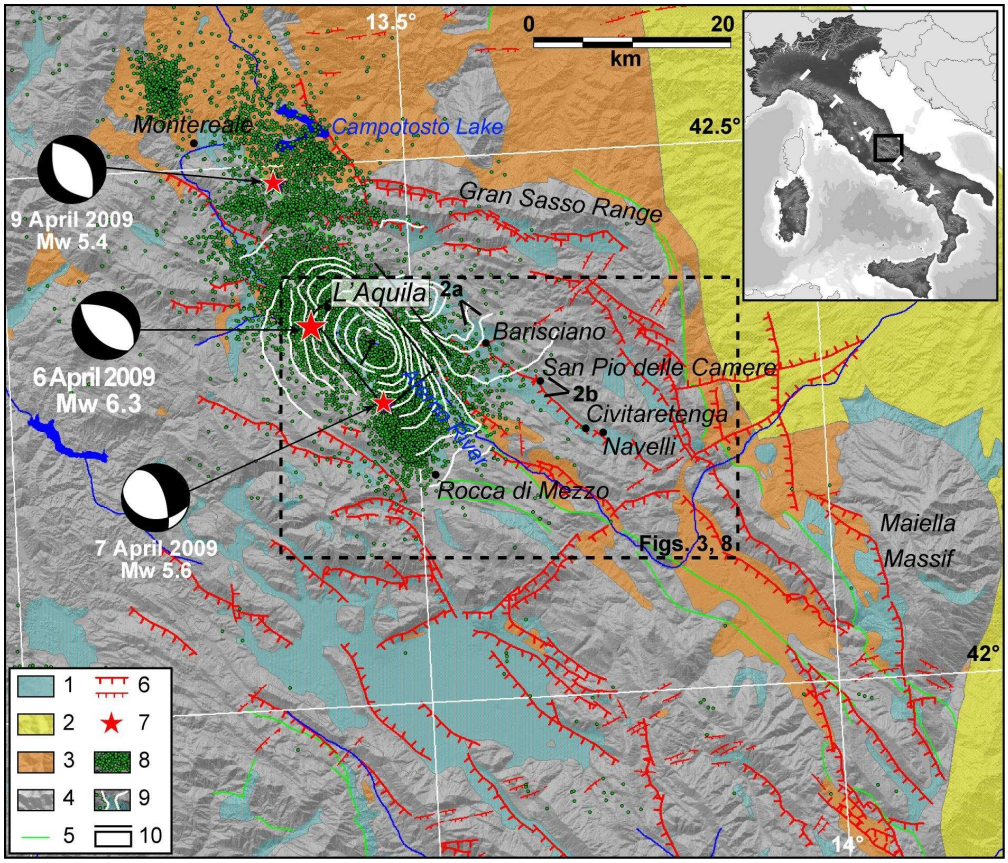

Simplified geological map of the Central Apennines (from Bigi et al., 1992; redrawn and modified). Legend: 1. Quaternary continental deposits; 2. Pliocene foredeep deposits; 3. Miocene foredeep deposits; 4. Meso-Cenozoic marine deposits of the Central Apennines chain; 5. Main thrust fronts; 6. active faults according to Vezzani and Ghisetti (1998; thin when uncertain); 7. Large star: 2009 mainshock epicenter; small stars: epicenters of largest aftershocks of 2009 sequence (ISIDe, 2010); 8. L'Aquila earthquake sequence (1 April-31 July, 2009; data from ISIDe, 2010); 9. Interferometric fringes illustrating elevation changes induced by the L'Aquila earthquake (from Walters et al., 2009, redrawn); 10. Surface projection of the mainshock fault rupture (from Table 1 in Walters et al., 2009, redrawn). 2a and 2b: view points of pictures in Fig. 2. Focal mechanisms of the mainshock and the two largest aftershocks are from Scognamiglio et al. (2010).
160x137mm (300 x 300 DPI)

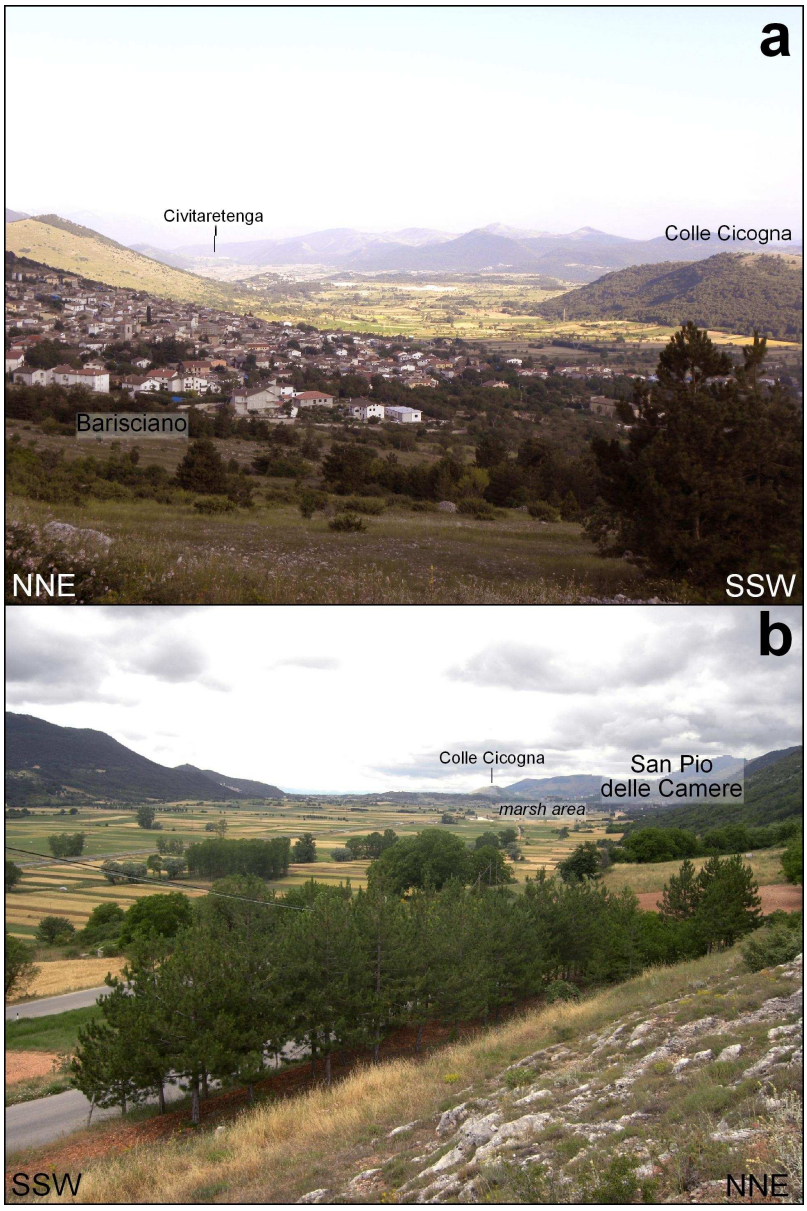

Views of the San Pio basin. a. Picture taken from the northwestern end of the basin, view to the southeast. b. Picture taken from the southeastern end of the basin, view to the northwest. See Fig. 1 for location of the view points.
165x247mm (300 x 300 DPI)

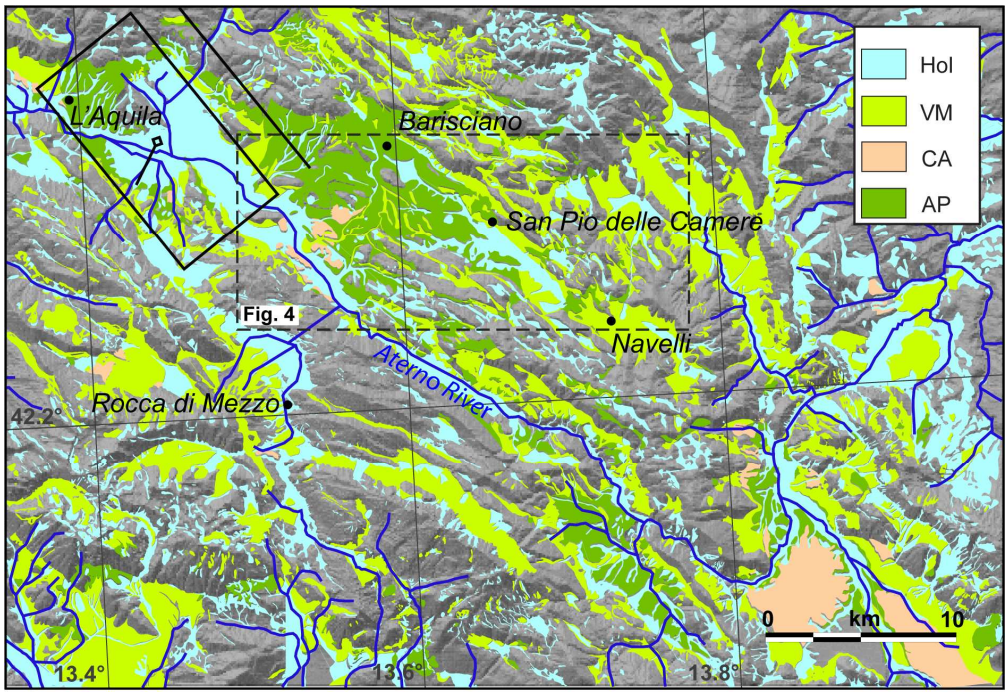

Geological setting of the study area (after Servizio Geologico d'Italia, 2006, redrawn and modified). Continental deposits: AP) Pliocene (?)-Middle Pleistocene; CA) latest Middle Pleistocene; VM) Upper Pleistocene; Hol) Holocene. Meso-Cenozoic bedrock is shown in grey. The black box represents the surface projection of the mainshock fault rupture (from Table 1 in Walters et al., 2009, redrawn). The continental Quaternary deposits filling the San Pio basin are characterized by different facies. Talus breccias and alluvial fans crop out along the surrounding slopes. Toward the valley, these facies are interfingered with fluvial and lacustrine sediments, which fill the lower part of the basin. Both the talus breccias and the alluvial fan deposits occasionally exhibit a very coarse clastic texture, in the latter case formed by well rounded pebbles, and are locally rather thick, up to tens of meters. Silts and clays instead prevail in the lacustrine facies.
159x109mm (300 x 300 DPI)

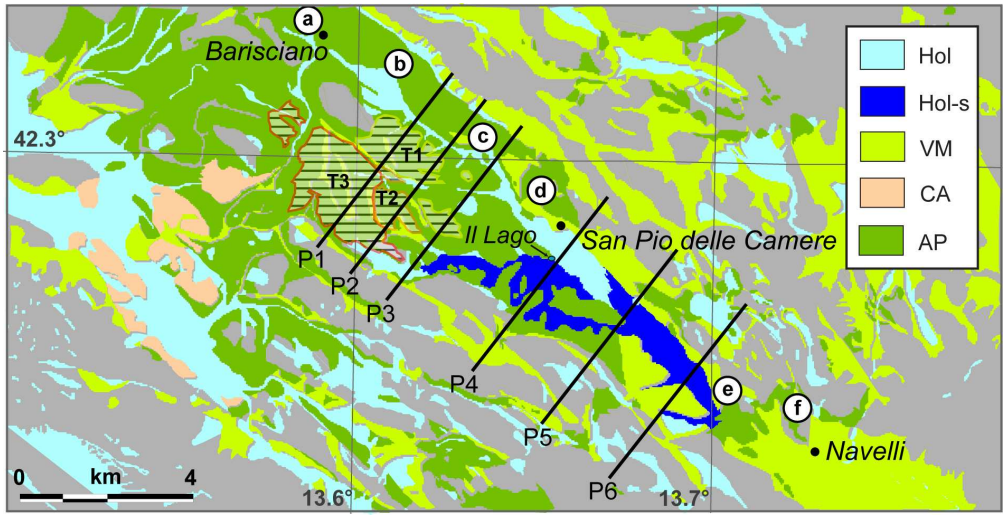

Detail of Fig. 3. Hol-s marks the Holocene lacustrine facies. Notice that these deposits are found only in the central part of the basin, near the current depocenter, supporting the hypothesis that subsidence has been a persisting feature throughout the Holocene. T1 to T3 are terraces at the top the AP deposits. Letters in white circles refer to the sites of structural analysis shown in Fig. 6.
160x82mm (300 x 300 DPI)

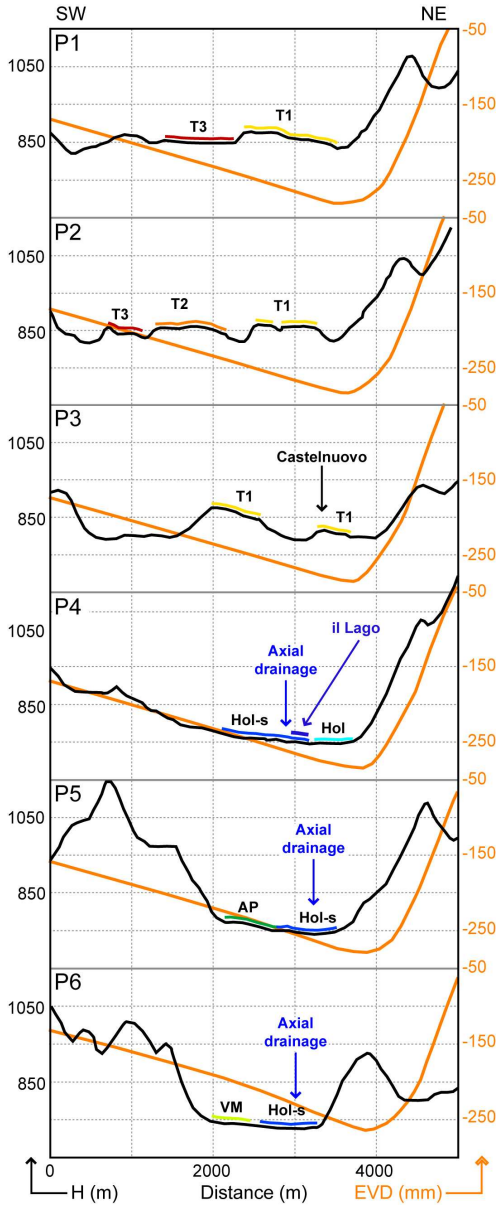

NNE-SSW-striking topographic profiles across the San Pio basin (traces in Fig. 4) and elevation changes due to 1 m of hypothetical slip over the model fault (in orange). Notice the asymmetry of the basin and the tilt towards NNE of the Pleistocene and Holocene surfaces, in accordance with the elevation changes predicted by the model. H: elevation a.s.l.; EVD: expected vertical displacement.
91x224mm (300 x 300 DPI)

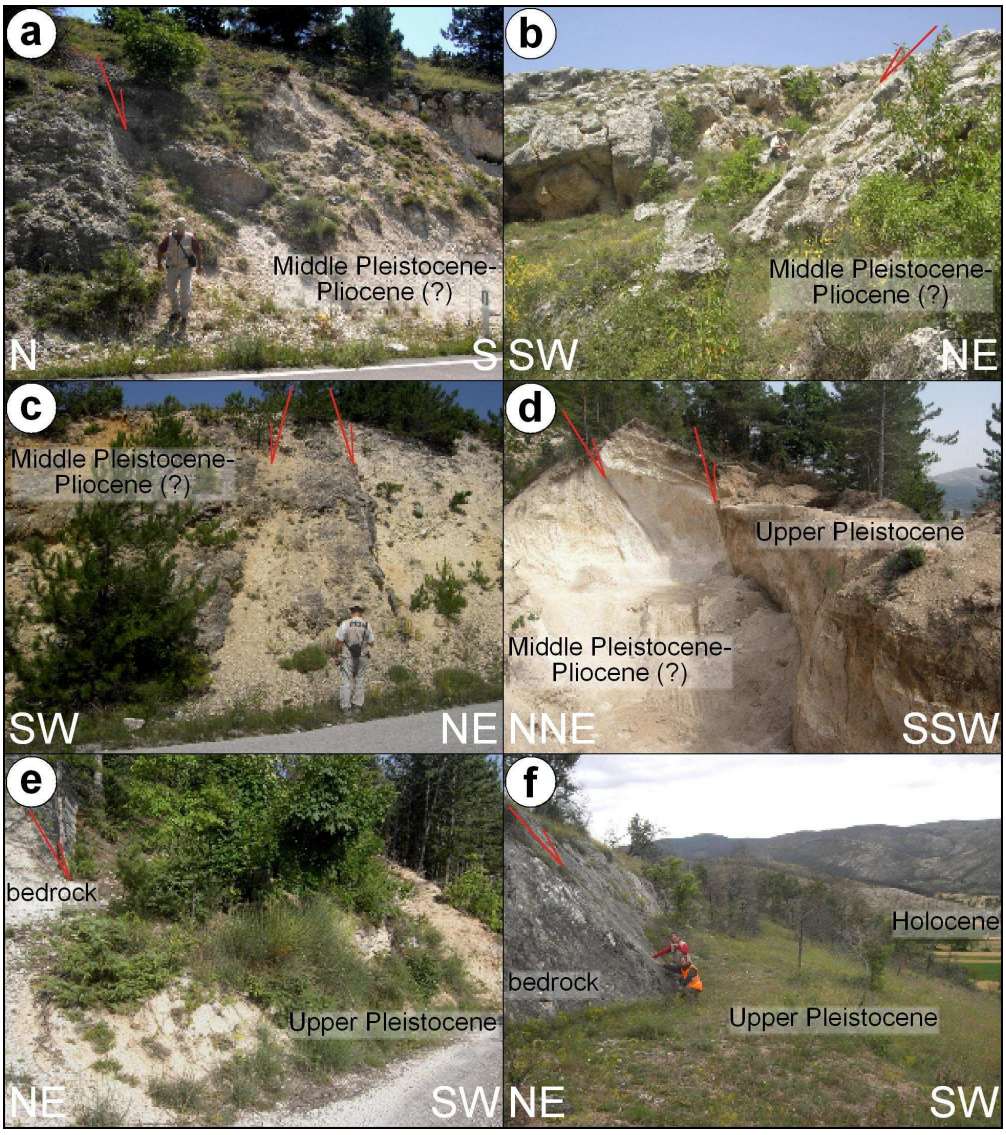

Faults (red arrows) and fractures along the slope bounding the San Pio basin to the NE. See Fig. 4 for location of the sites of observation. Pliocene (?)-Middle Pleistocene and Upper Pleistocene continental deposits overlying Jurassic and Cretaceous limestones (Servizio Geologico d'Italia, 2006) crop out extensively. The Pleistocene deposits exhibit slope talus facies, in many cases characterized by a coarse texture with large calcareous blocks, but in some instances show fluvial facies with well rounded pebbles.
165x185mm (300 x 300 DPI)

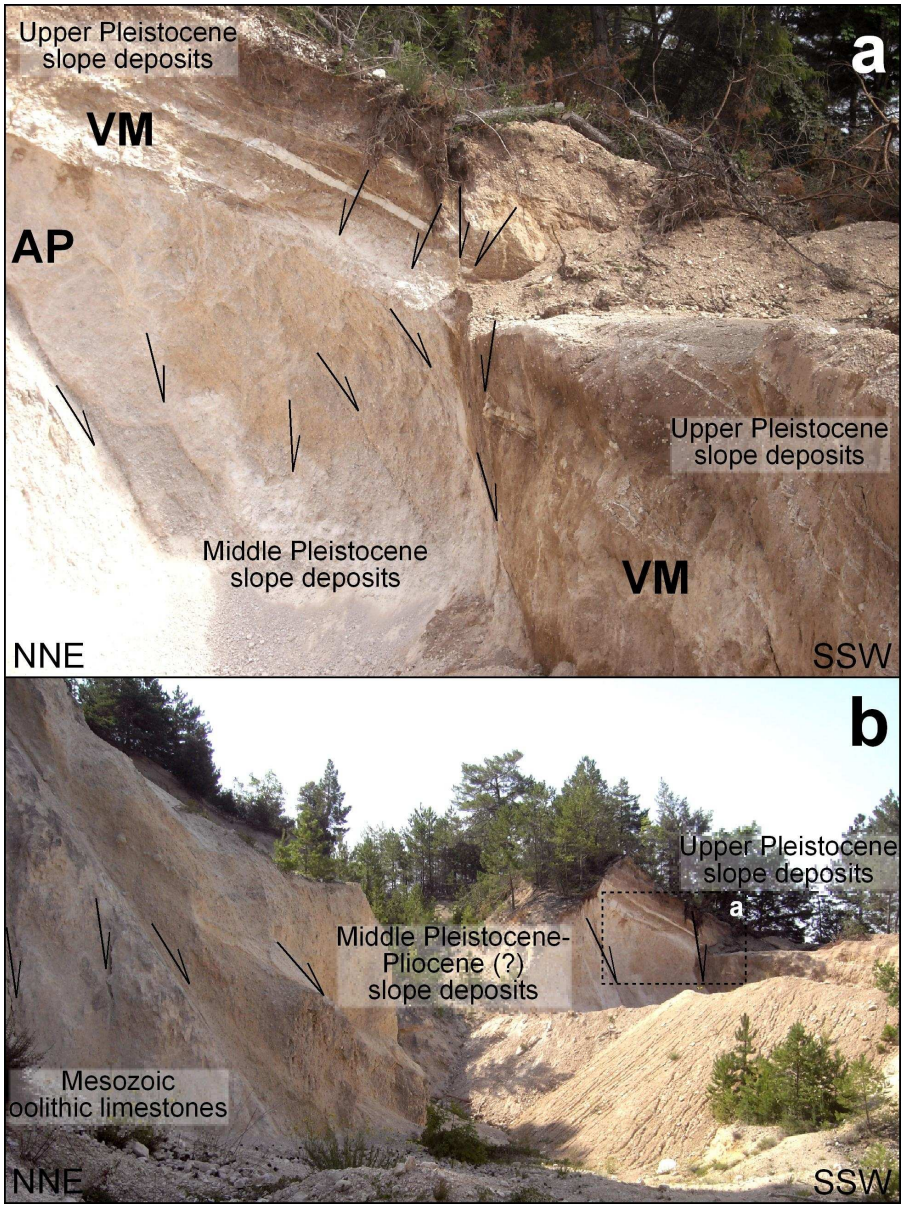

Active faults bounding the central part of the San Pio basin to the NE, near the village of San Pio delle Camere (detail of the site 6d in Fig. 6). The faults slipped during and after the deposition of both the Pliocene (?)-Middle Pleistocene deposits (AP) and the Upper Pleistocene (VM) deposits.
165x221mm (300 x 300 DPI)

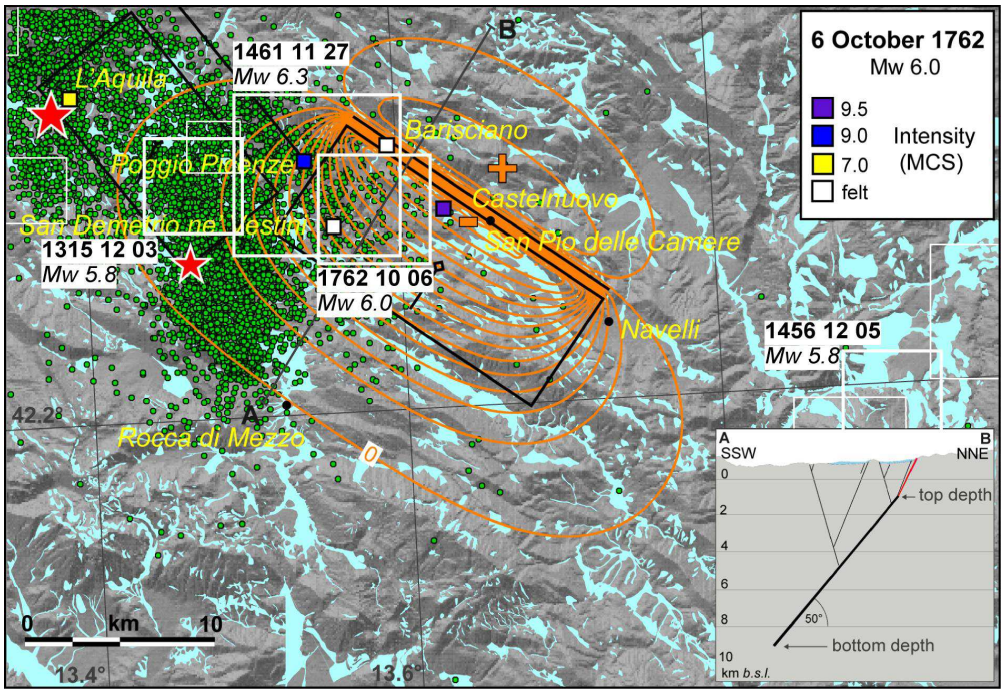

Plan view and cross-section of the seismogenic fault modeled for the San Pio basin (parameters in Table 1). Cross-section surface data from Servizio Geologico d'Italia (2006). The orange isolines show the expected elevation changes, in increments of 2 cm, resulting from 1 m of hypothetical unitary slip on the modeled fault (see also Fig. 5 for a cross-section view). Notice the good correspondence with basin geometry. The distribution of the L'Aquila aftershocks (green dots; ISIDe, 2010) and historical earthquakes (white squares; Guidoboni et al., 2007) is also shown. Red stars: epicenters of the mainshock and of the largest aftershock of the 2009 L'Aquila sequence. As an example, the damage distribution of the 1762 Aquilano earthquake is shown in MCS intensity scale.
160x109mm (300 x 300 DPI)